Supporting Information (SI) for:

Intramolecular Triplet-Triplet Annihilation Upconversion in 9,10-diphenylanthracene oligomers and dendrimers

Damir Dzebo[a], Karl Börjesson[b], Victor Gray[a], Kasper Moth-Poulsen[a], Bo Albinsson[a]*

[a]Chalmers University of Technology/Department of Chemistry and Chemical Engineering, 41296 Göteborg, Sweden
[b]University of Gothenburg/Department of Chemistry and Molecular Biology, 41296 Gothenburg

Table of Contents

Molar absorptivities

Table S1. Molar absorptivities of the studied compounds in toluene at the given wavelength

	PdOEP	DPA	Oligo	G1	G2
ε_{max} ($M^{-1}cm^{-1}$)	43 000[1]	12 500[2]	139 000	49 000[2]	101 000[2]
λ_{max} (nm)	547	375	401	399	401

[1]Ref (1), [2]Ref (2)

Stern-Volmer quenching

Samples containing PdOEP as the sensitizer and an increasing annihilator concentration were prepared and degassed though five freeze-pump-thaw cycles in a valve-sealed freeze-pumping cuvette or in melt-sealed sample tubes on a high-vacuum line. In Figure S1 the Stern-Volmer relation (eq. S1)

$$\frac{I_0}{I} = \frac{\tau_0}{\tau} = 1 + \tau_0 \, k_{TET1}[Q] \qquad \text{(S1)}$$

is fitted to the changes in PdOEP lifetimes. The expression holds true for dynamic quenching which is expected in the Liquid media where the sensitizer and the annihilator have no affinity to each other. The k_{TET1} is the rate constant of quenching or in this case Triplet Energy Transfer from the sensitizer to the annihilator.

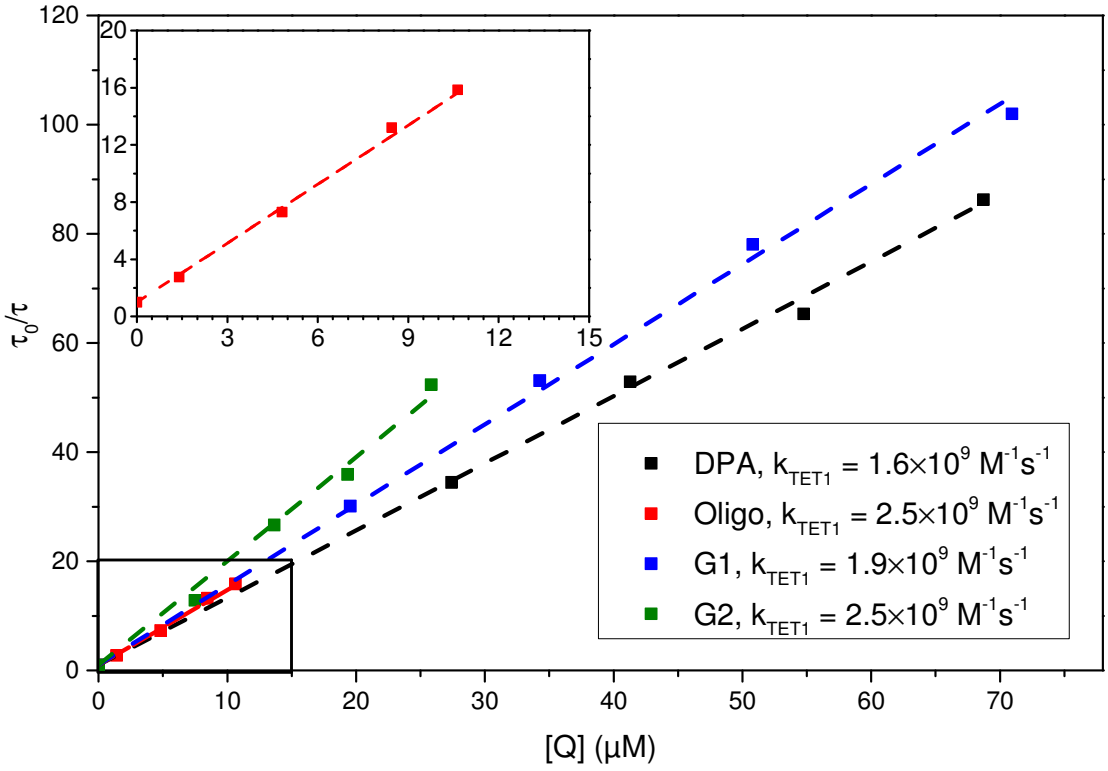

Figure S1. Stern-Volmer analysis of PdOEP in presence of DPA, Oligo, G1 and G2 as quencher (Q).

The lifetimes were measured on a Cary Eclipse Fluorescence Spectrophotometer with weak excitation pulses. The obtained k_{TET1} in toluene for PdOEP quenched by DPA, Oligo, G1 and G2 can be found in the legend and in Table 1. Unquenched sensitizer lifetimes in the four annihilator cases were determined to 770 μs, 555 μs, 765 μs and 765 μs respectively. Inset: magnification of the Oligo quenching analysis.

The difference in the unquenched sensitizer lifetimes is the result of the experimental series for the individual annihilators being conducted on separate occasions, resulting in slightly different deoxygenation efficiency. However, the deoxygenation procedure was unchanged within these experimental series and therefore the deoxygenation efficiency is not expected to fluctuate much for each individual annihilator type. This is supported by the good linear dependence in the Stern-Volmer analysis', as seen in Figure S1.

Sensitizer characterization

The PdOEP sensitizer triplet lifetime in toluene in absence of any annihilator was determined by capturing triplet emission traces at four different intensities, hence producing different amounts of triplets for each pumping intensity. This was performed using pulsed Nd:YAG Surlite nanosecond laser system (see Experimental). The following reactions (SR1-4) are expected to occur

$$^1S \xrightarrow{k_{exc}} {}^1S^* \qquad \text{Excitation (exc)} \qquad \text{(SR1)}$$

$$^1S^* \xrightarrow{k_{isc}} {}^3S^* \qquad \text{Inter-System Crossing (isc)} \qquad \text{(SR2)}$$

$$^3S^* + {}^3S^* \xrightarrow{k_{TTAS}} {}^1S + {}^1S^* \qquad \text{Triplet-Triplet Annihilation of sensitizer (TTAS)} \qquad \text{(SR3)}$$

$$^3S^* \xrightarrow{k_{PS}} {}^1S \qquad \text{Phosphorescence triplet decay of sensitizer (PS)} \qquad \text{(SR4)}$$

where S is the sensitizer, k is the rate constant of; excitation (exc), inter-system crossing (isc), Triplet-Triplet Annihilation between sensitizers (TTAS), and phosphorescence triplet decay of the sensitizer (PS). The kinetic description of the three forms of sensitizer in reactions (SR1-4) are:

$$\frac{d[S]}{dt} = k_{TTAS}\left[{}^3S^*\right]^2 + k_{PS}\left[{}^3S^*\right] - k_{exc}\left[{}^1S\right]_0 \qquad \text{(S2)}$$

$$\frac{d\left[{}^1S^*\right]}{dt} = -k_{isc}\left[{}^1S^*\right] + k_{TTAS}\left[{}^3S^*\right]^2 + k_{exc}\left[{}^1S\right]_0 \qquad \text{(S3)}$$

$$\frac{d\left[{}^3S^*\right]}{dt} = k_{isc}\left[{}^1S^*\right] - 2k_{TTAS}\left[{}^3S^*\right]^2 - k_{PS}\left[{}^3S^*\right] \qquad \text{(S4)}$$

Further, the rate of excitation[3] when using a monochromatic light source is

$$k_{exc} = P_{exc}(\lambda)\alpha(\lambda) \qquad \text{(S5)}$$

where $P_{exc}(\lambda)$ is the excitation photon flux in photons/cm^2/s and $\alpha(\lambda)$ is the absorption cross section of the sensitizer at the excitation wavelength in cm^2. The photon flux is further derived from the excitation power measured with a calibrated power meter and the beam diameter which was determined using a caliper and when possible also in combination with a laser alignment burn-paper. For the calculation of the photon flux and the rate of excitation in time-resolved measurements a 7 ns square pulse is assumed for simplicity.

The equations above were solved using the same methodology as with the time-resolved simulations (see section Simulations). For all the calculations the sensitizer inter-system crossing rate was set to $k_{isc} = 10^{12}\,s^{-1}$ as the PdOEP sensitizer forms triplets very efficiently[4].

The above kinetic model was fitted globally to the four decays as is illustrated in Figure S2. The average excitation intensity for the first and strongest decay was 14 mW and the rate constant k_{TTAS}, the lifetime $\tau = 1/k_{PS}$ and a scaling factor (relating excited state concentrations to oscilloscope readings in volt) were fit globally for the whole set.

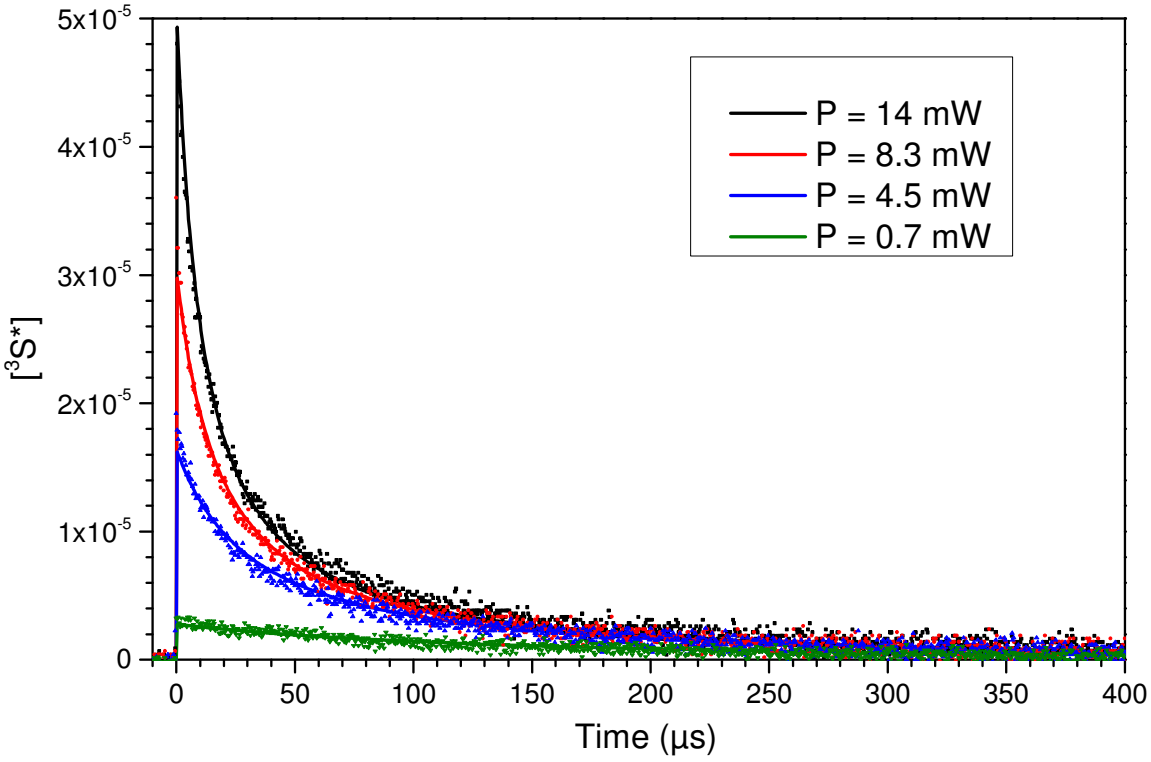

Figure S2. PdOEP excited triplet traces black to red at 665 nm captured at varying excitation intensities. Dotted lines are raw data and the solid lines are fits of the model.

The resulting fit was satisfactory and the obtained parameters are $k_{TTAS} = 1.75 \cdot 10^9$ $M^{-1}s^{-1}$ and $\tau_{PS} = 318\,\mu s$. The estimated triplet lifetime in toluene is a bit less than the reported 770 µs[4] suggesting that there may be some residual molecular oxygen in the sample.

The triplet lifetime of the sensitizer in solid PMMA matrix was recorded on a Cary Eclipse phosphorimeter with weak excitation pulses and was fit to a regular single exponential decay using a custom made MATLAB® program. The resulting fit is found in Figure S3. The obtained triplet lifetime was 1.58 ms which is in the same order of magnitude as reported[5] (1.90 ms in glass at 77 K).

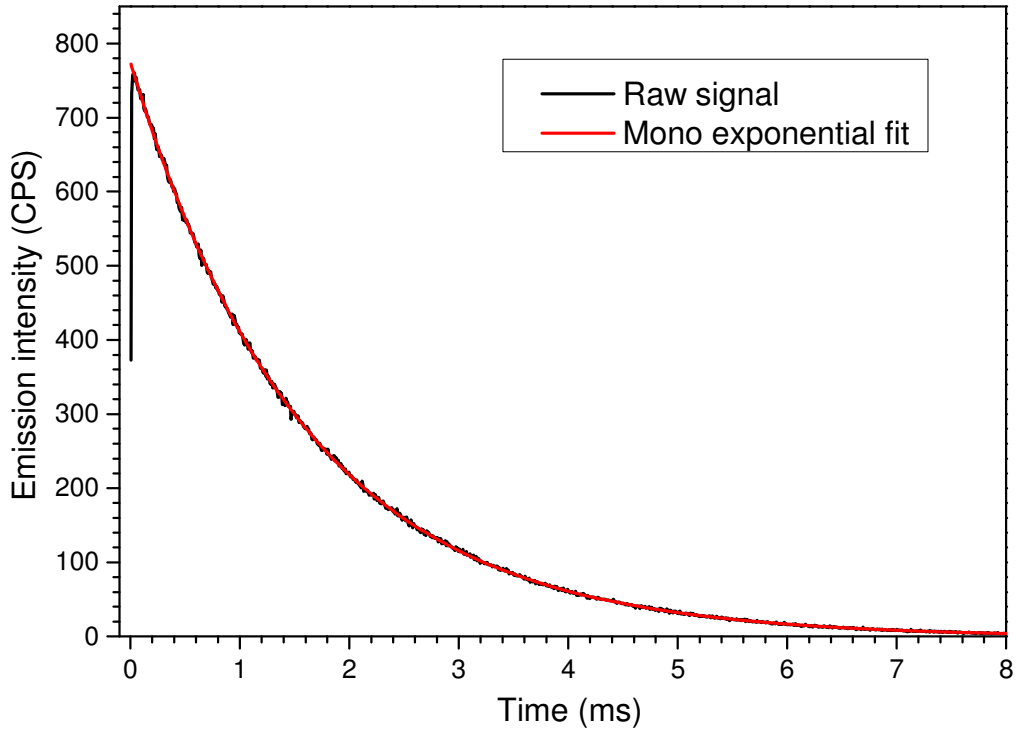

Figure S3. PdOEP emission decay in PMMA at room temperature. Concentration was 173 µM.

Annihilator characterization

The fluorescence decays of the annihilators in PMMA are found in Figure S4. Decays were recorded using TCSPC as described in Experimental section in the main text. The Oligomer fluorescence decay in argon degassed toluene is found in Figure S5 while the fluorescence decay data for the remaining samples are found in reference given in Table 1 in the main text. The triplet decay of the annihilators in PMMA is found in Figure S6.

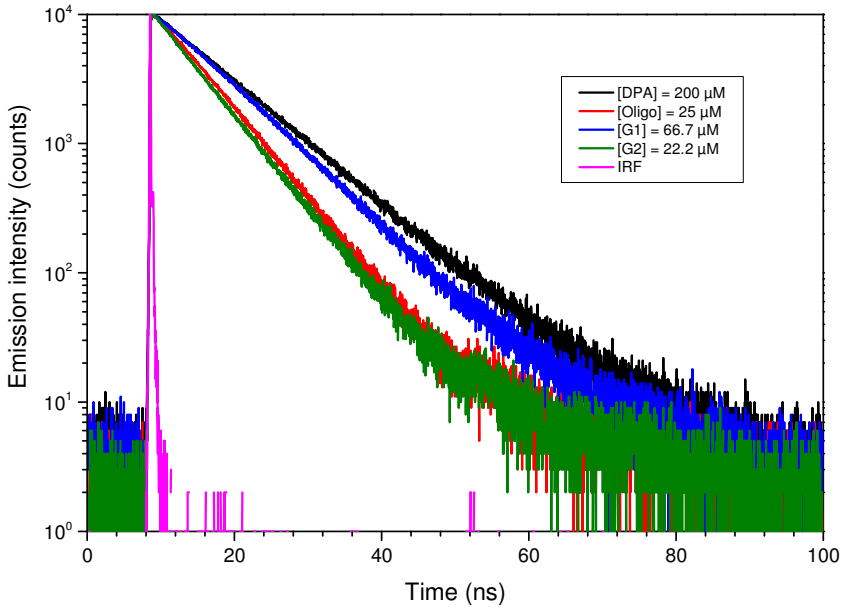

Figure S4. Annihilator fluorescence emission decays at 430 nm in PMMA. Recording made on picosecond laser system. The lifetime values are found in Table 1.

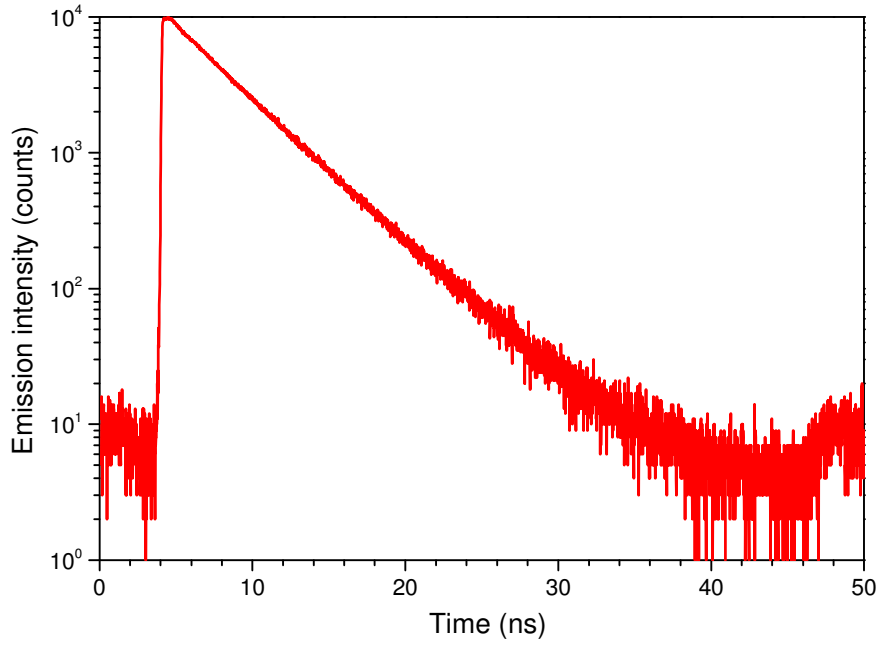

Figure S5. Oligo fluorescence emission decay in argon degassed toluene. The lifetime value is found in Table 1.

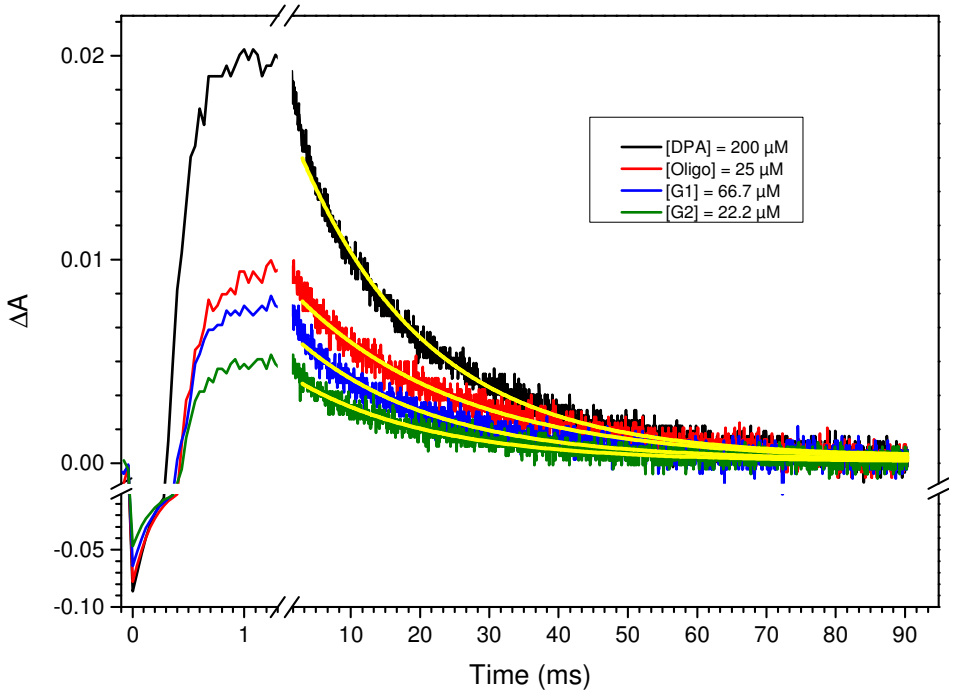

Figure S6. Annihilator transient absorption in PMMA at 420 nm captured on a nanosecond pulsed laser system by excitation at tripled fundamental Nd:YAG line (355 nm, 10 Hz, 7 ns FWHM pulse, average power 1.39 W and beam diameter of 8 mm). The high excitation power is necessary due to the annihilator's low ISC rate. Single-exponential tail fit of triplet transient absorption in yellow. Negative signal close to time zero is the delayed TTA-UC emission resulting from the intense excitation. The lifetime values are found in Table 1.

Simulations and Fitting

The simulations are based on reactions SR1-10.

$^3S^* + {}^1A \xrightarrow{k_{TET1}} {}^1S + {}^3A^*$	Primary Triplet Energy Transfer to ground state annihilator (TET1)	(SR5)
$^3A^* + {}^3A^* \xrightarrow{k_{TTA1}} {}^1A + {}^1A^*$	Primary (*inter*molecular) Triplet-Triplet Annihilation (TTA1)	(SR6)
$^3A^* \xrightarrow{k_{PA}} {}^1A$	Excited triplet decay of annihilator (PA)	(SR7)
$^3S^* + {}^3A^* \xrightarrow{k_{TET2}} {}^1S + {}^3A^{**}$	Secondary Triplet Energy Transfer to triplet excited annihilator (TET2)	(SR8)
$^3A^{**} \xrightarrow{k_{TTA2}} {}^1A^*$	Secondary (*intra*molecular) Triplet-Triplet Annihilation (TTA2)	(SR9)
$^1A^* \xrightarrow{k_{FA}} {}^1A$	Excited singlet decay of annihilator (FA)	(SR10)

Time-resolved simulations of the Oligo, G1 and G2 are based on the following equations (S6-S12) where for the DPA monomer eq. (S10) is removed along with all secondary energy transfer terms (TET2 and TTA2) and associated species ($^3A^{**}$).

$$\frac{d[^1S]}{dt} = k_{TTAS}[^3S^*]^2 + k_{PS}[^3S^*] + k_{TET1}[^3S^*][^1A] + k_{TET2}[^3S^*][^3A^*] - k_{exc}[^1S] \quad (S6)$$

$$\frac{d[^1S^*]}{dt} = -k_{isc}[^1S^*] + k_{TTAS}[^3S^*]^2 + k_{exc}[^1S]_0 \quad (S7)$$

$$\frac{d[^3S^*]}{dt} = k_{isc}[^1S^*] - 2k_{TTAS}[^3S^*]^2 - k_{PS}[^3S^*] - k_{TET1}[^3S^*][^1A] - k_{TET2}[^3S^*][^3A^*] \quad (S8)$$

$$\frac{d[^3A^*]}{dt} = k_{TET1}[^3S^*][^1A] - 2k_{TTA1}[^3A^*]^2 - k_{TET2}[^3S^*][^3A^*] - k_{PA}[^3A^*] \quad (S9)$$

$$\frac{d[^3A^{**}]}{dt} = k_{TET2}[^3S^*][^3A^*] - k_{TTA2}[^3A^{**}] \quad (S10)$$

$$\frac{d[^1A^*]}{dt} = k_{TTA1}[^3A^*]^2 - k_{FA}[^1A^*] + k_{TTA2}[^3A^{**}] \quad (S11)$$

$$\frac{d[^1A]}{dt} = -k_{TET1}[^3S^*][^1A] + k_{TTA1}[^3A^*]^2 + k_{FA}[^1A^*] + k_{PA}[^3A^*] \quad (S12)$$

In the equations (S6-S12) A is the annihilator and the ** indicates double-excited species. The rate constants are explained in reactions SR1-10.

The steady-state simulations for the Oligo, G1 and G2 are based on equations (S13-S19) and for the DPA monomer eq. (S17) is removed along with all secondary energy transfer terms (TET2 and TTA2) and associated species ($^3A^{**}$).

$$0 = [^1S] + [^1S^*] + [^3S^*] - [^1S]_0 \qquad \text{S balance} \qquad (S13)$$

$$0 = -k_{isc}[^1S^*] + k_{TTAS}[^3S^*]^2 + k_{exc}[^1S] \qquad ^1S^* \qquad (S14)$$

$$0 = k_{isc}[^1S^*] - 2k_{TTAS}[^3S^*]^2 - k_{PS}[^3S^*] - k_{TET1}[^3S^*][^1A] - k_{TET2}[^3S^*][^3A^*] \qquad ^3S^* \qquad (S15)$$

$$0 = k_{TET1}[^3S^*][^1A] - 2k_{TTA1}[^3A^*]^2 - k_{TET2}[^3S^*][^3A^*] - k_{PA}[^3A^*] \qquad ^3A^* \qquad (S16)$$

$$0 = k_{TET2}[^3S^*][^3A^*] - k_{TTA2}[^3A^{**}] \qquad ^3A^{**} \qquad (S17)$$

$$0 = k_{TTA1}[^3A^*]^2 - k_{FA}[^1A^*] + k_{TTA2}[^3A^{**}] \qquad ^1A^* \qquad (S18)$$

$$0 = [^3A^*] + [^3A^{**}] + [^1A^*] + [^1A] - [^1A]_0 \qquad \text{A balance} \qquad (S19)$$

Steady-state and time-resolved simulations were performed using MATLAB® 2015b (MathWorks®). For each of the two simulations a global correction factor, *cf*, was implemented to scale the recorded emission data (I_{raw}) to the simulated emission given in eq. (S20)

$$I_{sim} = [^1A^*]\Phi_{FA} \qquad (S20)$$

where I_{sim} is the simulated emission, $[^1A^*]$ is the single excited annihilator concentration and Φ_{FA} is the fluorescence quantum yield of the annihilator.

The parameters for simulations in Liquid media were fitted to both steady-state and time-resolved data simultaneously. The parameters for simulations in Solid media were fitted only to steady-state data for reasons given in the main text.

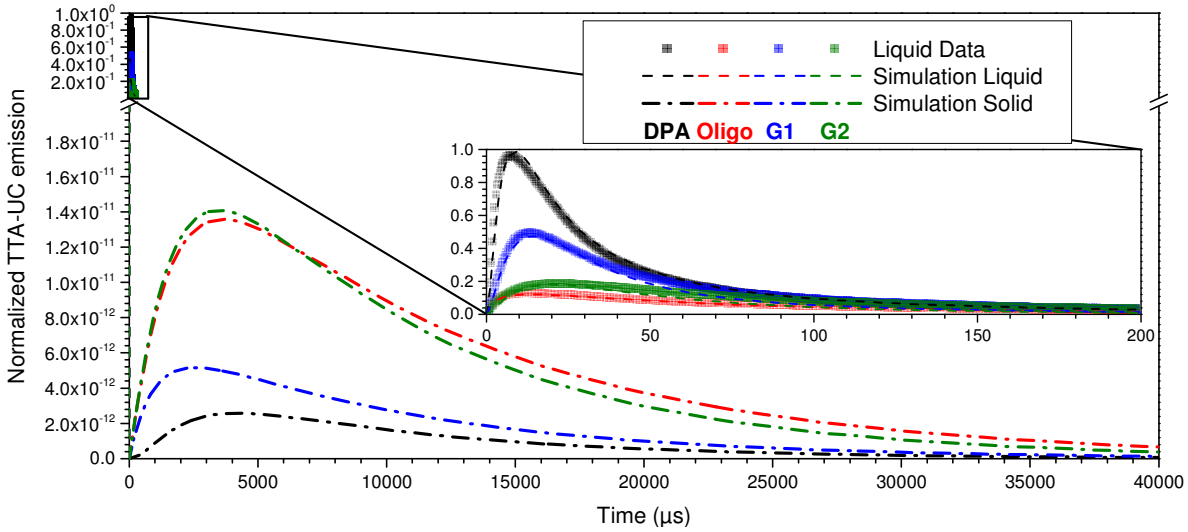

Figure S7. Simulated time-resolved UC emission using parameters from the steady-state fit in Solid media. Inset: Magnification of the time-resolved data in Liquid media and simulations from Figure 3b illustrating the expected difference in intensity and kinetics.

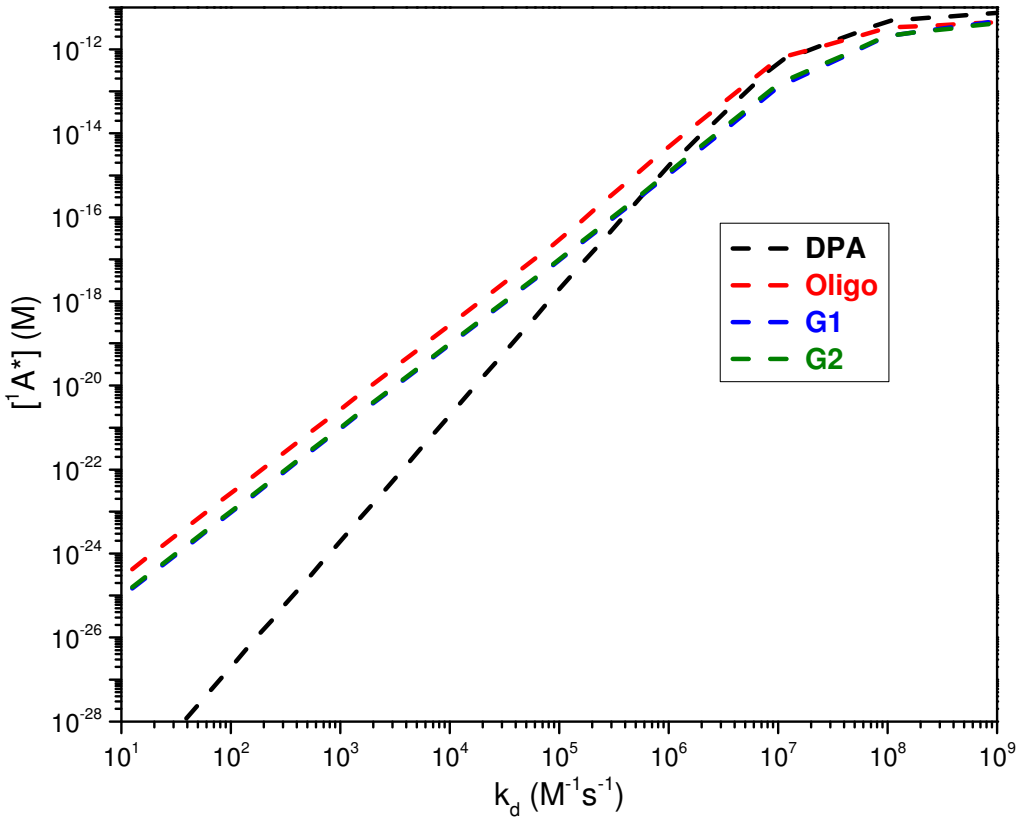

Figure S8: Same simulation as in Figure 4 but with all annihilator concentrations at 200μM to illustrate the removal of the higher molecular concentration effect of DPA seen in Figure 2 at low viscosities.

Excitation intensity dependence

The different trend regions in steady-state UC emission can be isolated using equations S14-S18 as follows:

From (S15) we have that

$$k_{isc}\left[^1S^*\right] - 2k_{TTAS}\left[^3S^*\right]^2 - k_{PS}\left[^3S^*\right] - k_{TET\,2}\left[^3S^*\right]\left[^3A^*\right] = k_{TET\,1}\left[^3S^*\right]\left[^1A\right] \quad \text{(S21)}$$

and from (S16)

$$2k_{TTA1}\left[^3A^*\right]^2 + k_{TET\,2}\left[^3S^*\right]\left[^3A^*\right] + k_{PA}\left[^3A^*\right] = k_{TET\,1}\left[^3S^*\right]\left[^1A\right] \quad \text{(S22)}$$

By combining (S21) and (S22) one obtains

$$k_{isc}\left[^1S^*\right] - 2k_{TTAS}\left[^3S^*\right]^2 - k_{PS}\left[^3S^*\right] - k_{TET\,2}\left[^3S^*\right]\left[^3A^*\right] = 2k_{TTA1}\left[^3A^*\right]^2 + k_{TET\,2}\left[^3S^*\right]\left[^3A^*\right] + k_{PA}\left[^3A^*\right] \quad \text{(S23)}$$

Further we assign that

$$k_{exc}\left[^1S\right] = I_{exc} \quad \text{(S24)}$$

and in combination with (S14) we have that

$$-k_{TTAS}\left[^3S^*\right]^2 + I_{exc} = k_{isc}\left[^1S^*\right] \quad \text{(S25)}$$

Finally we also have from (S17) that

$$k_{TET\,2}\left[^3S^*\right]\left[^3A^*\right] = k_{TTA2}\left[^3A^{**}\right] \quad \text{(S26)}$$

By combining (S23) with (S25) and (S26) we obtain

$$I_{exc} - 3k_{TTAS}\left[^3S^*\right]^2 - k_{PS}\left[^3S^*\right] = 2k_{TTA1}\left[^3A^*\right]^2 + 2k_{TTA\,2}\left[^3A^{**}\right] + k_{PA}\left[^3A^*\right] \quad \text{(S27)}$$

We also assign

$$I_{UC} = k_{FA}\left[^1A^*\right]\Phi_{FA} \quad \text{(S28)}$$

and in combination with (S18) we have that

$$I_{UC} = k_{FA}\left[^1A^*\right]\Phi_{FA} = \Phi_{FA}\left(k_{TTA\,1}\left[^3A^*\right]^2 + k_{TTA\,2}\left[^3A^{**}\right]\right) \quad \text{(S29)}$$

For the annihilation dominant region (linear) we assume from (S27) that

$$k_{TTA1}\left[^3A^*\right]^2 + k_{TTA2}\left[^3A^{**}\right] >> \frac{k_{PA}\left[^3A^*\right]}{2} \quad \text{(S30)}$$

we obtain the "Linear" dependence of TTA-UC as

$$I_{UC,Lin} = \Phi_{FA}\left(\frac{I_{exc} - 3k_{TTAS}\left[^3S^*\right]^2 - k_{PS}\left[^3S^*\right]}{2}\right) \quad \text{(S31)}$$

However for the lower excitation intensities we have that

$$k_{TTA1}\left[^3\mathrm{A}^*\right]^2 + k_{TTA2}\left[^3\mathrm{A}^{**}\right] << \frac{k_{PA}\left[^3\mathrm{A}^*\right]}{2} \tag{S32}$$

and thus the "Quadratic" dependence is

$$I_{UC,Quad} = \Phi_{FA}\left(k_{TTA1}\left(\frac{I_{exc} - 3k_{TTAS}\left[^3\mathrm{S}^*\right]^2 - k_{PS}\left[^3\mathrm{S}^*\right]}{k_{PA}}\right)^2 + k_{TTA2}\left[^3\mathrm{A}^{**}\right]\right) \tag{S33}$$

At this point it is clear that the "Linear" and "Quadratic" components given in eqs. (S31) and (S33) are not of pure linear and quadratic nature due to the presence of $\left[^3\mathrm{S}^*\right]$ which is proportional to the excitation intensity. Since in Solid media, the "Linear" and "Quadratic" components never actually cross at high excitation intensities due to the perturbing sensitizer ground state bleach, trend components are projected from the non-perturbed regions (Figure S9, gray lines) to establish the expected thresholds. We therefore obtain the numerical threshold by extrapolating the non-bleach-perturbed regions of eqs. (S31) and (S33) and find the crossing point. The photon flux threshold is obtained using equations (S24) and (S5) and is illustrated by vertical solid lines in Figure S9.

For a fluid and ideally prepared TTA-UC system the secondary processes (TET2 and TTA2) are not active, see main text. Further the triplet-excited sensitizer is quenched efficiently by the annihilator (TET1), thus the deactivation paths through phosphorescence (PS) and self-annihilation (TTAS) are negligible. With these approximations equations (S31) and (S33) are reduced to the familiar components of truly linear and quadratic nature as

$$I_{UC,Lin}^{ideal} = \Phi_{FA}\left(\frac{I_{exc}}{2}\right) \tag{S34}$$

and

$$I_{UC,Quad}^{ideal} = \Phi_{FA}\, k_{TTA1}\left(\frac{I_{exc}}{k_{PA}}\right)^2. \tag{S35}$$

By equating the two ideal components the ideal threshold intensity is obtained as

$$I_{exc}^{ideal} = \frac{{k_{PA}}^2}{2k_{TTA1}} \tag{S36}$$

which is rewritten in terms of photon flux using equations (S24) and (S5) to give

$$P_{exc}^{Th,Ideal} = \frac{{k_{PA}}^2}{2k_{TTA1}\cdot\alpha\left[^1S\right]} \tag{S37}$$

and is illustrated in Figure S9 as vertical dash-dot lines for comparison with the numerically obtained threshold photon flux. The threshold values obtained through both methods are found in Table S2 for numerical comparison. As can be observed the ideal approximations hold well in the Liquid media but not as well in the Solid media.

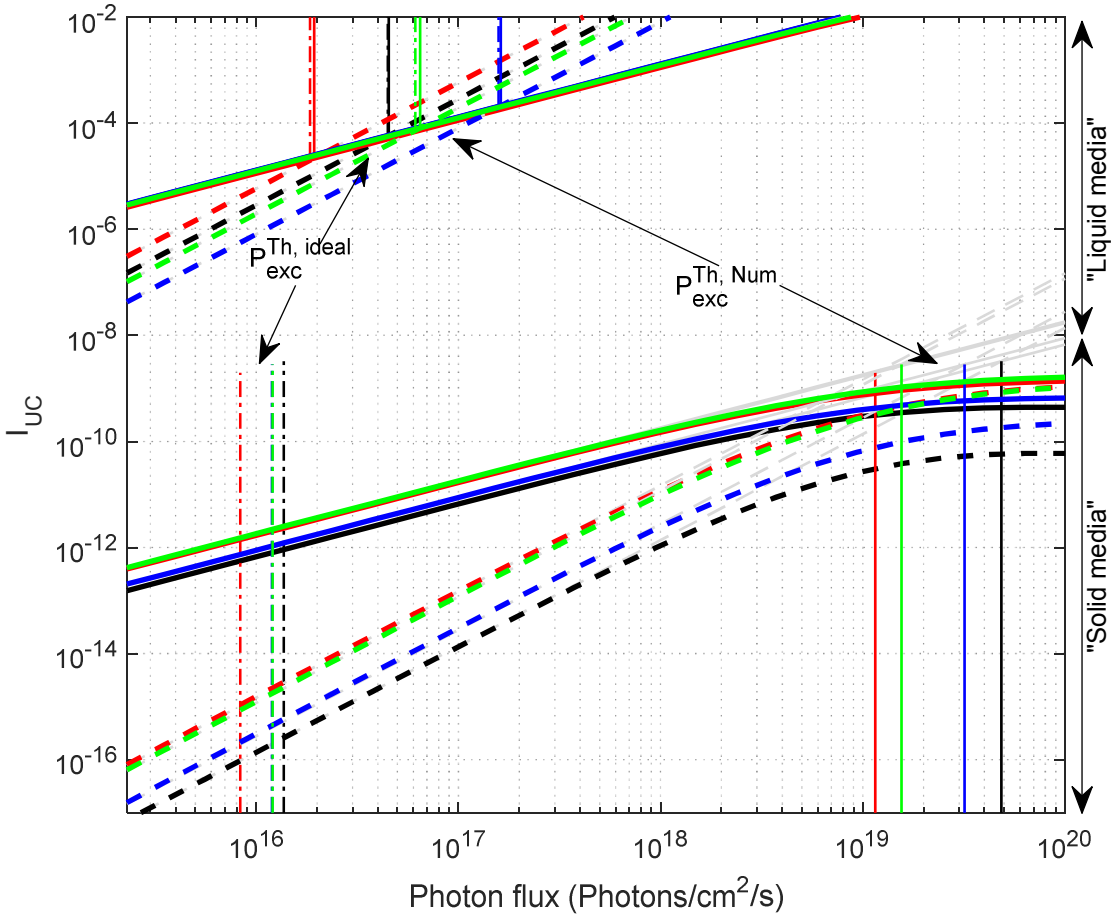

Figure S9: Threshold components of "Linear" and "Quadratic" dependence as solid and dashed lines, respectively. UC emission intensity above10^{-8} is done in Liquid media and below in Solid media. The colors Black, Red, Blue and Green represent samples with DPA, Oligo, G1 and G2, respectively. Gray lines represent projection of the corresponding threshold components along the non-perturbed regions. Vertical dash-dot and solid lines represent the ideal and numerical thresholds respectively.

Table S2. Threshold values in Liquid- and Solid media extrapolated numerically and calculated through ideal approximations as well as the difference between the two illustrating the large inaccuracy of the ideal approximation in the Solid media.

	Liquid media (Toluene)				Solid media (PMMA)			
(photons/cm^2/s) $\times 10^{-17}$	**DPA$_{Liquid}$**	**Oligo$_{Liquid}$**	**G1$_{Liquid}$**	**G2$_{Liquid}$**	**DPA$_{Solid}$**	**Oligo$_{Solid}$**	**G1$_{Solid}$**	**G2$_{Solid}$**
$P_{exc}^{Th,Num}$	0.452	0.194	1.62	0.647	485	115	318	156
$P_{exc}^{Th,Ideal}$	0.448	0.185	1.58	0.612	0.137	0.083	0.120	0.121
Difference	0.004	0.009	0.040	0.035	485	115	318	156

DPA oligomer synthesis analysis

Peak Results

	Mn	Mw	MP	Polydispersity
1	2795	3298	3100	1.179946

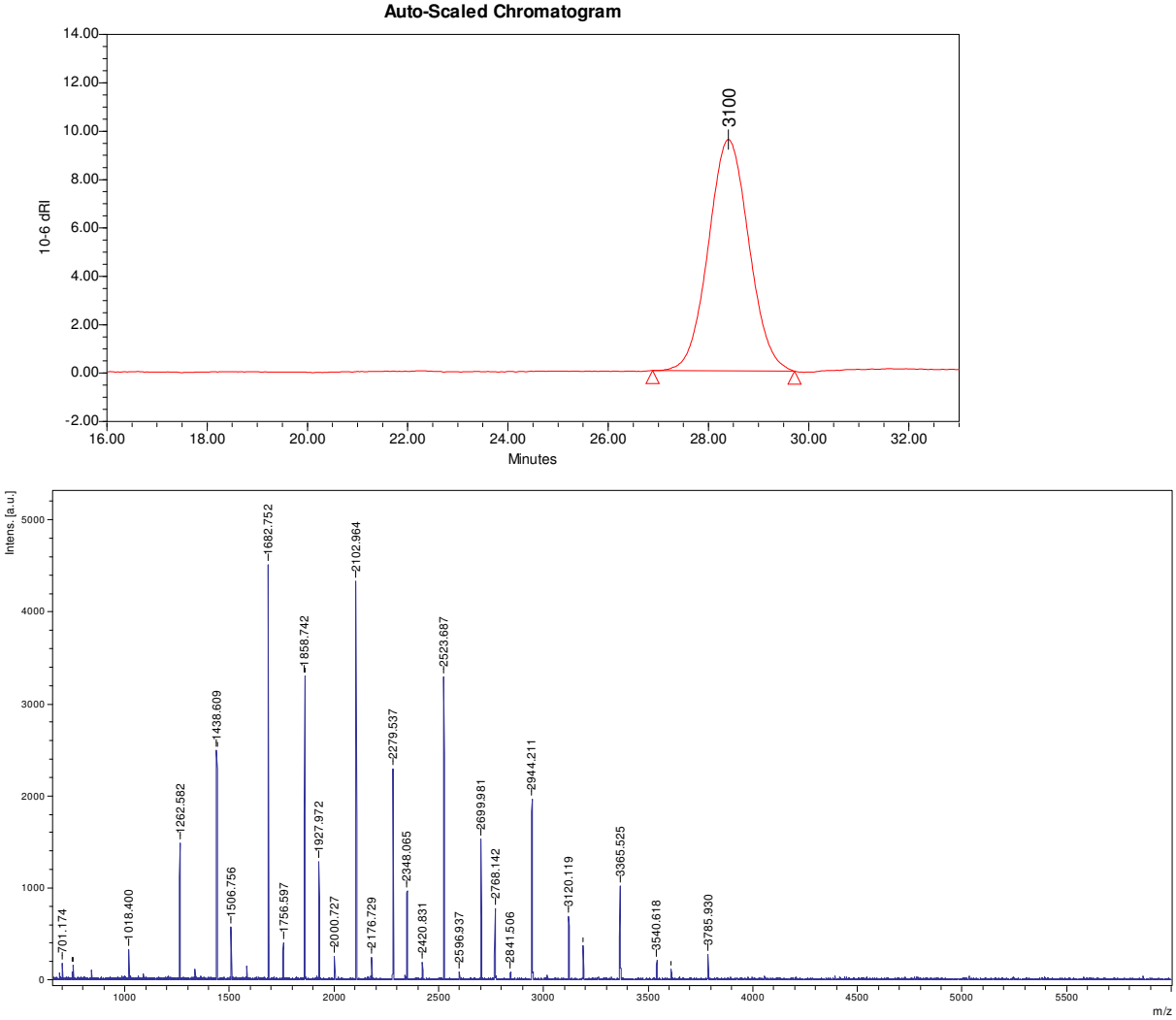

Figure S10. Size exclusion chromatogram (top) and mass spectrum (bottom, MALDI) of DPA oligomer.

Investigation of possible intermolecular interactions in Solid media

Emission lifetime of PdOEP in the different PMMA samples with and without the annihilators is found in Figure S11 where all samples display monoexponential decay kinetics with the same lifetime (~1.6 ms). In the hypothetical case of significant amounts of sensitizer-annihilator complexes we would have expected to find different and likely non-monoexponential decays of the different samples. Since this is not the case, we conclude that no such interaction exist.

Possible dimers of the PdOEP sensitizer would have been expected to produce deviation from the regular PdOEP emission spectrum, especially at higher concentrations and in PMMA. To investigate possible presence of such dimers, steady-state emission measurements further into the red region of the sensitizer spectra were performed. The emission envelope of the dissolved sensitizer in toluene at low concentration and the same from the employed PMMA samples (173 μM PdOEP) is found in Figure S12. The envelope of the emission is almost identical between the PMMA samples and the low concentration solution sample. Additionally an even higher concentration of PdOEP in PMMA also displays no deviation from the envelope of the low concentration solution sample. This suggests that there are no dimer formations in the PMMA samples up to and including the employed PdOEP concentrations.

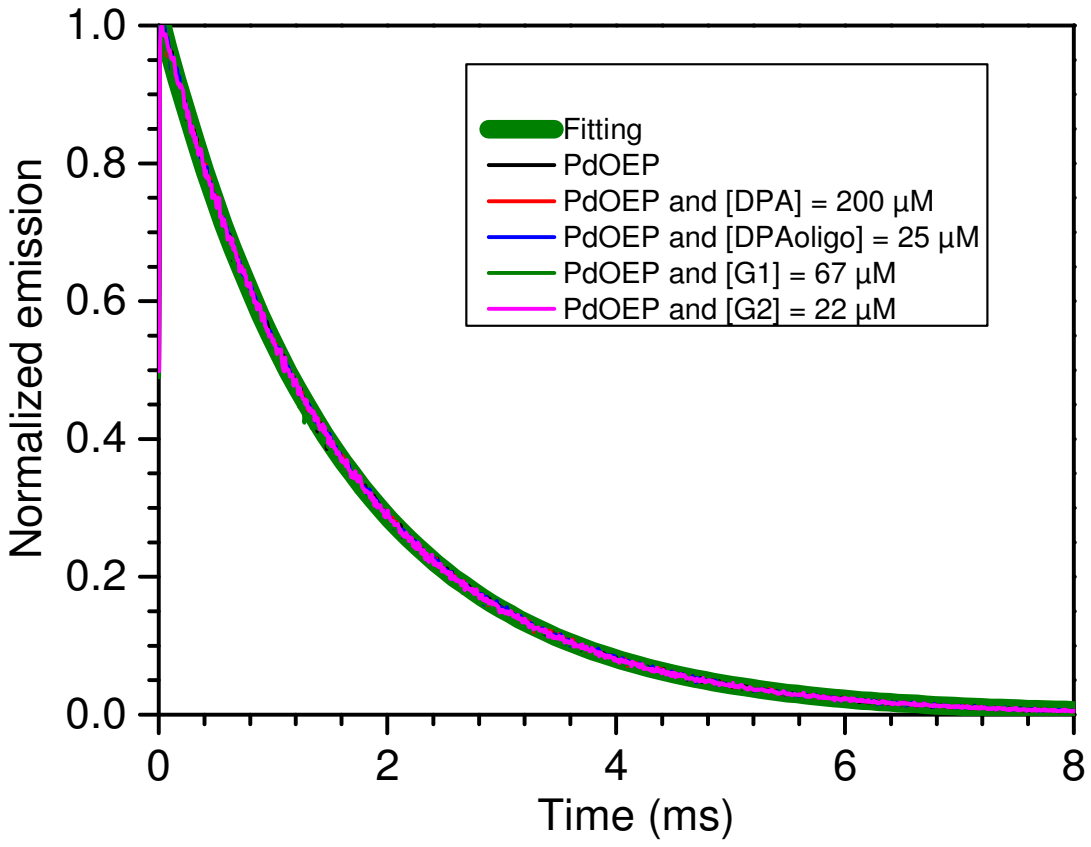

Figure S11. Time-resolved PdOEP (173 μM) emission decay in PMMA without and with annihilators. All decays overlap almost perfectly. Mono exponential fit results in the same lifetime of 1.58 ms (~1.6 ms) for all traces.

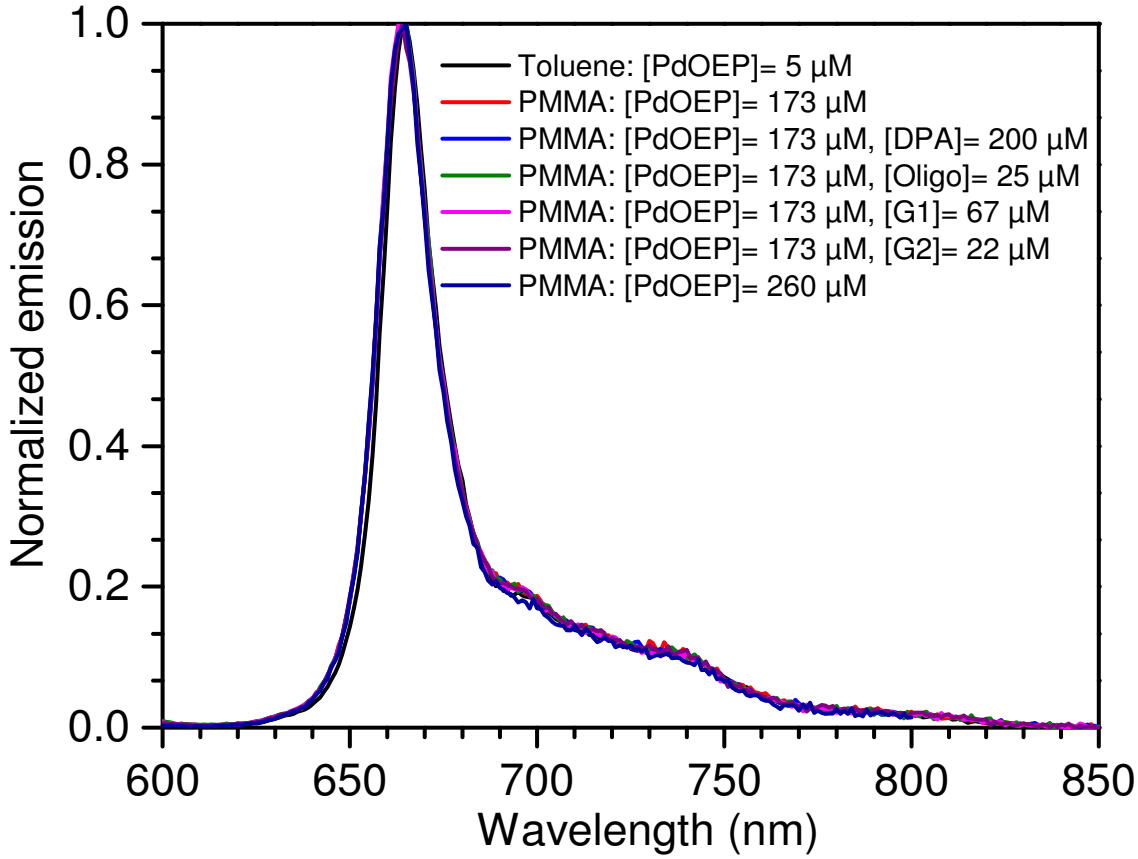

Figure S12. Emission spectra of PdOEP; 5 µM in toluene (as in Figure 2), all used PMMA samples (173 µM) including a control-sample with only PdOEP without annihilator and a higher concentration control sample in PMMA.

References

(1) Stolzenberg, A. M.; Schussel, L. J., Synthesis, Characterization, and Electrochemistry of Copper(Ii) and Palladium(Ii) Hydroporphyrins: The Copper(I) Octaethylisobacteriochlorin Anion. *Inorg. Chem.* **1991**, *30*, 3205-3213.
(2) Borjesson, K.; Gilbert, M.; Dzebo, D.; Albinsson, B.; Moth-Poulsen, K., Conjugated Anthracene Dendrimers with Monomer-Like Fluorescence. *Rsc Adv* **2014**, *4*, 19846-19850.
(3) Schmidt, T. W.; Castellano, F. N., Photochemical Upconversion: The Primacy of Kinetics. *J. Phys. Chem. Lett.* **2014**, *5*, 4062-4072.
(4) Amao, Y., Probes and Polymers for Optical Sensing of Oxygen. *Microchimica Acta* **2003**, *143*, 1-12.
(5) Singh, A.; Johnson, L. W., Phosphorescence Spectra and Triplet State Lifetimes of Palladium Octaethylporphyrin, Palladium Octaethylchlorin and Palladium 2,3-Dimethyloctaethylisobacteriochlorin at 77 K. *Spectrochimica Acta Part A: Molecular and Biomolecular Spectroscopy* **2003**, *59*, 905-908.